Author/s:
Hauke, J;Riessland, M;Lunke, S;Eyüpoglu, IY;Blümcke, I;El-osta, A;Wirth, B;Hahnen, E

Title:
Survival motor neuron gene 2 silencing by DNA methylation correlates with spinal muscular atrophy disease severity and can be bypassed by histone deacetylase inhibition

Date:
2009-01-05

Citation:
Hauke, J., Riessland, M., Lunke, S., Eyüpoglu, I. Y., Blümcke, I., El-osta, A., Wirth, B. & Hahnen, E. (2009). Survival motor neuron gene 2 silencing by DNA methylation correlates with spinal muscular atrophy disease severity and can be bypassed by histone deacetylase inhibition. Human Molecular Genetics, 18 (2), pp.304-317. https://doi.org/10.1093/hmg/ddn357.

Persistent Link:
https://hdl.handle.net/11343/257118

*Human Molecular Genetics, 2009, Vol. 18, No. 2* ***304–317***
*doi:10.1093/hmg/ddn357*
*Advance Access published on October 29, 2008*

# *Survival motor neuron gene 2* silencing by DNA methylation correlates with spinal muscular atrophy disease severity and can be bypassed by histone deacetylase inhibition

**Jan Hauke[1,2,3], Markus Riessland[1,2,3], Sebastian Lunke[4], Ilker Y. Eyüpoglu[5], Ingmar Blümcke[6], Assam El-Osta[4], Brunhilde Wirth[1,2,3] and Eric Hahnen[1,2,3,*]**

[1]Institute of Human Genetics, [2]Institute of Genetics, [3]Center for Molecular Medicine Cologne (CMMC), University of Cologne, Cologne, Germany, [4]Epigenetics in Human Health and Disease, Baker IDI Heart and Diabetes Institute, Melbourne, Victoria, Australia, [5]Department of Neurosurgery and [6]Department of Neuropathology, University of Erlangen, Erlangen, Germany

Received July 22, 2008; Revised and Accepted October 26, 2008

**Spinal muscular atrophy (SMA), a common neuromuscular disorder, is caused by homozygous absence of the *survival motor neuron gene 1* (*SMN1*), while the disease severity is mainly influenced by the number of *SMN2* gene copies. This correlation is not absolute, suggesting the existence of yet unknown factors modulating disease progression. We demonstrate that the *SMN2* gene is subject to gene silencing by DNA methylation. *SMN2* contains four CpG islands which present highly conserved methylation patterns and little interindividual variations in *SMN1*-deleted SMA patients. The comprehensive analysis of *SMN2* methylation in patients suffering from severe versus mild SMA carrying identical *SMN2* copy numbers revealed a correlation of CpG methylation at the positions −290 and −296 with the disease severity and the activity of the first transcriptional start site of *SMN2* at position −296. These results provide first evidence that *SMN2* alleles are functionally not equivalent due to differences in DNA methylation. We demonstrate that the methyl-CpG-binding protein 2, a transcriptional repressor, binds to the critical *SMN2* promoter region in a methylation-dependent manner. However, inhibition of *SMN2* gene silencing conferred by DNA methylation might represent a promising strategy for pharmacologic SMA therapy. We identified histone deacetylase (HDAC) inhibitors including vorinostat and romidepsin which are able to bypass *SMN2* gene silencing by DNA methylation, while others such as valproic acid and phenylbutyrate do not, due to HDAC isoenzyme specificities. These findings indicate that DNA methylation is functionally important regarding SMA disease progression and pharmacological *SMN2* gene activation which might have implications for future SMA therapy regimens.**

## INTRODUCTION

Autosomal recessive proximal spinal muscular atrophy (SMA) is a severely progressing neuromuscular disorder and a major cause of inherited childhood lethality. SMA is characterized by the loss of lower motor neurons in the anterior horns of the spinal cord, causing symmetrical weakness and atrophy of voluntary muscles. Patients with SMA have been classified into four types depending on age of onset and progression of the disease: type I SMA is the most severe form with generalized muscle weakness and hypotonia and a disease onset within the first 6 months of life. The children are unable to sit or walk and usually die within the first 2 years of life. Type II SMA individuals are able to sit but unable to walk

*To whom correspondence should be addressed at: Institute of Human Genetics, University of Cologne, Kerpener Str. 34, 50931 Cologne, Germany. Tel: +49 22147886464; Fax: +49 22147886465; Email: eric.hahnen@uk-koeln.de

unaided. They usually present first symptoms after the first 6 months of life and survive beyond 2 years. Type III SMA patients are able to sit and walk, and the lifespan is not reduced. Disease onset before the age of 3 years is classified as type IIIa, whereas an age of onset beyond 3 years is classified as type IIIb SMA. Type IV SMA patients are mildly affected with an age of onset after the third decade of life (reviewed in 1).

The disease determining *survival motor neuron gene 1* (*SMN1*) is homozygously absent in 96% of all SMA patients and intragenic *SMN1* mutations are rare (2). Within the SMA region on chromosome 5q, the human *survival motor neuron* (*SMN*) *gene* exists in two copies, *SMN1* and *SMN2*, which are ubiquitously expressed and encode identical proteins (3). Even though all SMA patients lacking *SMN1* carry at least one *SMN2* gene copy, the amount of functional SMN protein produced by *SMN2* is not sufficient to prevent progressive α-motor neuron degeneration. This finding has been assigned to a single translationally silent 'C' to 'T' transition within exon 7, affecting the splicing of primary *SMN* transcripts (4). As a consequence, the disease determining *SMN1* gene produces full-length transcripts only (FL-*SMN*), whereas the majority of *SMN2* transcripts lack exon 7 due to alternative splicing (Δ7-*SMN*). Truncated Δ7-SMN proteins are reduced in their ability to self-oligomerize, which is essential for proper SMN function (5,6), and have been shown to ameliorate, but not to prevent, the SMA phenotype *in vivo* (7). However, several studies have revealed a strong inverse correlation between the number of *SMN2* copies and SMA severity (8–11). Most type I SMA patients carry two *SMN2* copies, whereas type II SMA patients carry three and type III SMA patients carry three or four *SMN2* copies. Rarely, patients with two *SMN2* copies show mild phenotypes (9), suggesting the influence of yet unidentified modifying factors modulating disease progression. Due to the disease modifying property of the *SMN2* gene which has been verified in transgenic mouse models (12), *SMN2* represents the major therapeutic target. Consequently, transcriptional *SMN2* activation and/or modulation of the *SMN2* splicing pattern to increase FL-*SMN* levels may be an effective strategy for SMA treatment.

Numerous small-molecule histone deacetylase (HDAC) inhibitors have been shown to increase *SMN2*-derived FL-SMN protein levels *in vitro* by transcriptional activation and/or by modulation of the *SMN2* splicing pattern. These compounds include the fatty acids sodium butyrate (SB), phenylbutyrate (PB) and valproic acid (VPA) (13–17); the benzamide M344 (15,18) as well as the hydroxamic acids SAHA and trichostatin A (TSA) (15,19,20). The potential applicability of HDAC inhibitors for SMA therapy was confirmed in transgenic mice which mimic SMA-like features. By employing a knockout transgenic mouse model, Chang *et al*. (17) demonstrated that oral application of SB increased lifespan and *SMN2*-derived SMN protein levels in motor neurons of affected mice. Concordantly, Tsai *et al*. (21) demonstrated that oral application of VPA attenuates motor neuron death, increases spinal SMN protein levels and partially normalizes motor function in SMA-like mice. Clinical phase II trials have been initiated to evaluate the efficacy of the FDA-approved drugs PB and VPA for SMA therapy. Pilot trials with small numbers of patients treated with PB (22,23) or VPA (24,25) revealed elevated *FL-SMN2* transcript levels in some patients and increased quantitative muscle strength and subjective muscle function, which might further emphasize the potential use of HDAC inhibitors for SMA treatment.

However, the efficacies of PB and VPA for SMA therapy await clinical confirmation and the mechanism(s) by which HDAC inhibitors elevate transcriptional *SMN2* gene activity remain elusive. In general, HDAC inhibition promotes a more relaxed chromatin structure, allowing transcriptional activation. Given the fact that the fundamental mechanisms of epigenetic gene regulation, histone modification and DNA methylation have shown to be intimately interlinked (26,27), we hypothesized that DNA methylation plays a pivotal role in epigenetic *SMN2* gene regulation and SMA pathogenesis. DNA methylation has been shown to be the most stable type of epigenetic modification modulating the transcriptional plasticity of mammalian genomes (28). However, the role of DNA methylation in *SMN2* gene regulation has not been addressed so far. In this study, we demonstrate for the first time that the *SMN2* gene is subject to gene silencing by DNA methylation, which might have major implications for SMA disease progression and upcoming pharmacological interventions for epigenetic SMA therapy.

## RESULTS

### *SMN2* gene activity is reduced by DNA methylation

We raised the question whether the major target gene for SMA therapy, *SMN2*, is subject to gene silencing mediated by DNA methylation. To address this issue, *SMN1*-deleted fibroblast cell lines (ML5, ML16) derived from two independent SMA patients carrying three *SMN2* copies were treated with various doses of 5-aza-2′-deoxycytidine (Aza), a well-established DNA-demethylating compound. Aza treatment increased *SMN2*-derived transcript and protein levels in a dose-dependent fashion in both SMA fibroblast cell lines (Fig. 1A and B), indicating that *SMN2* gene activity is inversely correlated with DNA methylation. Using both cell lines, we previously have shown that HDAC inhibitors augment SMN2 protein levels by transcriptional *SMN2* gene activation and increased *SMN2* exon 7 inclusion (14,15,18). Concordantly, treatment of SMA fibroblasts (ML16) with effective doses of the experimental pan-HDAC inhibitor M344 significantly increased total *SMN2* transcript levels (Fig. 1C). However, even though interference with either DNA methylation or HDAC activity was sufficient to increase *SMN2* gene expression, there is no additive or synergistic effect when combined (Fig. 1C).

### *SMN2* is a methylated gene containing four CpG islands

To identify putative CpG islands (CGIs) involved in epigenetic *SMN2* gene regulation by DNA methylation, we analysed the genomic region 3000 nucleotides (nt) upstream and downstream of the translational *SMN2* start site (defined as nt position +1). By employing the CGI finder algorithm (www.EBI.ac.uk/emboss) we identified four putative CGIs

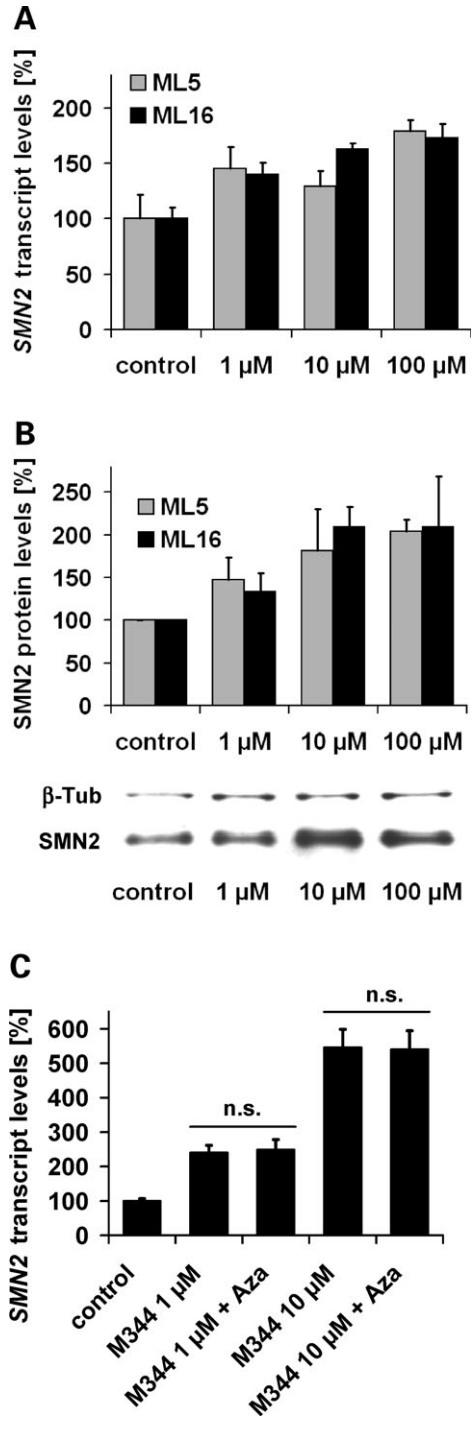


**Figure 1.** Transcriptional *survival motor neuron gene 2* (*SMN2*) activation by the DNA-demethylating drug 5-aza-2′-deoxycytidine (Aza) in *SMN1*-deleted SMA (spinal muscular atrophy) fibroblasts. Bar graphs show *SMN2* transcript (**A**) and SMN2 protein levels (**B**) in ML5 and ML16 fibroblast cell lines treated with various doses of Aza for 72 h (mean ± SEM). Expression levels in solvent- and time-matched controls were set to 100%. Increased *SMN2* transcript levels (normalized to ß-actin) were observed following Aza treatment (1, 10, 100 μM) and a dose-dependent *SMN2* gene activation was confirmed on protein level (normalized to ß-tubulin). A representative western blot analysis (ML16) is shown. (**C**) Quantification of *SMN2* transcript levels (normalized to ß-actin) in ML16 cells after treatment with different doses of the *SMN2*-activating HDAC (histone deacetylase) inhibitor M344 either alone or in combination with 10 μM Aza for 48 h. Transcriptional *SMN2* gene activation either by M344 alone or in combination with Aza (10 μM) reached levels of significance in all cases ($P < 0.05$, *t*-test). A >5-fold induction was observed following treatment with 10 μM M344 (546 ± 53%), while no additive effects were observed after co-treatment with 10 μM Aza ($P > 0.05$, *t*-test).

that localize within a ∼2 kb genomic region (nt −896 to +1146) surrounding the translational *SMN2* start site (Fig. 2A). These four putative CGIs, subsequently referred to as $^{SMN2}$CGIs, contain a total of 85 CpG dinucleotides, 14 of which are located in $^{SMN2}$CGI 1 (nt −896 to −645), 12 in $^{SMN2}$CGI 2 (nt −469 to −247), 38 in $^{SMN2}$CGI 3 (nt −151 to +295) and 21 in $^{SMN2}$CGI 4 (nt +844 to +1146). To quantify DNA methylation levels of each CpG dinucleotide located within the four $^{SMN2}$CGIs, we performed bisulphite genomic sequencing using pyrosequencing technology (29). The method is based on the selective deamination of unmethylated cytosine to uracil by treatment with bisulphite, while 5-methylcytosine remains unchanged. Pyrosequencing of subsequently generated PCR (polymerase chain reaction) products allows for both the detection and the quantification of cytosine methylation. Using genomic DNA isolated from *SMN1*-deleted SMA fibroblasts (ML5, ML16), bisulphite genomic sequencing revealed almost identical *SMN2* methylation patterns in both SMA fibroblast cell lines (Fig. 2B). $^{SMN2}$CGI 1 and $^{SMN2}$CGI 4 were hypermethylated in both cell lines with mean methylation levels >70%. $^{SMN2}$CGI 3 was hypomethylated (mean methylation levels <10%) with a single outlier at nt position +89, while $^{SMN2}$CGI 2 displayed intermediate mean methylation levels. Using bisulphite-treated DNA derived from ML5 and ML16 SMA fibroblasts as templates, cloning and sequencing of PCR products revealed similar results. Again, $^{SMN2}$CGI 1 and $^{SMN2}$CGI 4 were almost completely methylated, $^{SMN2}$CGI 3 was nearly unmethylated (data not shown), while $^{SMN2}$CGI 2 showed intermediate methylation levels (Fig. 2C).

### *SMN2* gene methylation patterns are highly conserved and correlate with SMA severity

The vast majority of *SMN1*-deleted SMA patients carrying two *SMN2* copies suffer from type I or II SMA, while only few patients (∼2%) develop a mild (type III SMA) phenotype (9), suggesting the existence of a yet unknown factor counteracting disease progression. To address whether *SMN2* gene methylation correlates with the disease severity, we analysed methylation levels of each CpG dinucleotide within the $^{SMN2}$CGIs using DNA isolated from blood samples taken from 10 unrelated, *SMN1*-deleted type I SMA patients carrying two *SMN2* copies (six females, four males). Bisulphite genomic sequencing identified *SMN2* methylation patterns similar to those observed in SMA fibroblasts (Fig. 3A), suggesting that *SMN2* gene methylation patterns do not essentially differ between tissues. Again, $^{SMN2}$CGI 1 and $^{SMN2}$CGI 4 appeared to be hypermethylated, $^{SMN2}$CGI 3 hypomethylated with a single outlier at position +89, while $^{SMN2}$CGI 2 displayed intermediate mean methylation levels. An unexpected observation was that methylation levels of each single CpG dinucleotide showed only little

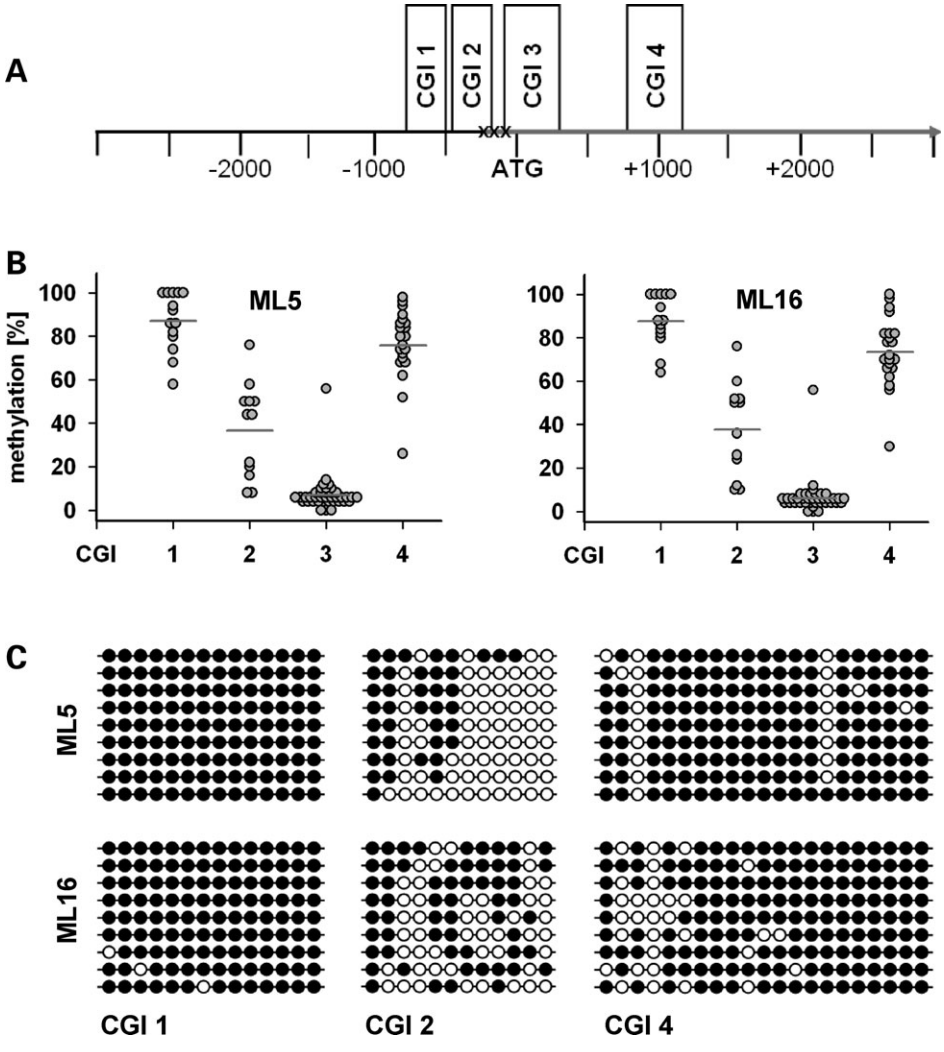


**Figure 2.** *Survival motor neuron gene 2* (*SMN2*) is a methylated gene containing four CpG islands (CGIs). Putative CGIs within the genomic region 3000 nucleotides (nt) upstream and downstream the translational *SMN2* start site (NCBI36: 5:70254287:70248287) were identified using the CGI finder and plotting tool (www.EBI.ac.uk/emboss). This algorithm identified four putative CGIs within the respective genomic region ($^{SMN2}$CGI 1: nt −896 to −645, $^{SMN2}$CGI 2: nt −469 to −247, $^{SMN2}$CGI 3: nt −151 to +295, $^{SMN2}$CGI 4: nt +844 to +1146). $^{SMN2}$CGI 2 contains the first out of three transcriptional start sites (TSS) of *SMN2* at nt −296, while the second TSS at nt position −242 is located close to the downstream border of $^{SMN2}$CGI 2 (30,31). (**A**) Schematically illustrates the localizations of all four $^{SMN2}$CGIs within the analysed genomic region. The localizations of the TSS at nt positions −296, −242 and −163 are indicated (30,31). (**B**) Frequency plots illustrating the methylation levels of each CpG dinucleotide within each $^{SMN2}$CGI in the respective SMA(Spinal muscular atrophy)-fibroblasts. The mean methylation levels of each $^{SMN2}$CGI, indicated by a horizontal line, are as follows: ML5: $^{SMN2}$CGI 1: 87.1%, $^{SMN2}$CGI 2: 36.6%, $^{SMN2}$CGI 3: 6.9%, $^{SMN2}$CGI 4: 75.9%; ML16: $^{SMN2}$CGI 1: 87.7%, $^{SMN2}$CGI 2: 37.7%, $^{SMN2}$CGI 3: 6.2%, $^{SMN2}$CGI 4: 73.4%. (**C**) Methylation analysis of $^{SMN2}$CGI 1, $^{SMN2}$CGI 2 and $^{SMN2}$CGI 4 in ML5 and ML16 fibroblasts cell lines by bisulphite treatment, followed by PCR amplification of the respective $^{SMN2}$CGI, cloning of PCR products, and sequencing. The methylation patterns of nine independent clones for each $^{SMN2}$CGI and each cell line are shown. Empty circles represent unmethylated CpGs, whereas full circles correspond to their methylated status.

interindividual variations between the 10 type I SMA patients (Fig. 3A). The subsequent analysis of DNA isolated from blood samples taken from seven available *SMN1*-deleted type III SMA patients carrying two *SMN2* copies (four females, three males) again revealed little interindividual variations (Fig. 3B). However, the comparison of methylation levels of each CpG dinucleotide identified significant correlations between CpG methylation levels and the disease severity at seven CpGs located in $^{SMN2}$CGI 1 (nt −871, −695), $^{SMN2}$CGI 2 (nt −296, −290), and $^{SMN2}$CGI 4 (nt +855, +988, +1103) (Fig. 3C). At six sites (nt −871, −695, −296, −290, +855, +1103), significantly lower methylation frequencies were observed in type III compared with type I SMA patients. A striking finding at this point was that the most pronounced differences in CpG methylation levels were observed at nt position −296 ($^{SMN2}$CGI 2; type I SMA: $94.1 \pm 6.3\%$; type III SMA: $66.7 \pm 8.0\%$, $P = 0.000084$, *t*-test), which exactly represents the first out of three transcriptional start sites (TSS) of *SMN2* (Fig. 2A) (30,31). The correlation of CpG methylation levels of all 17 patients with their gender (10 females, seven males) did not reveal any significant results (data not shown), which is in line with a previous comprehensive study showing that DNA methylation is not affected by gender (28).

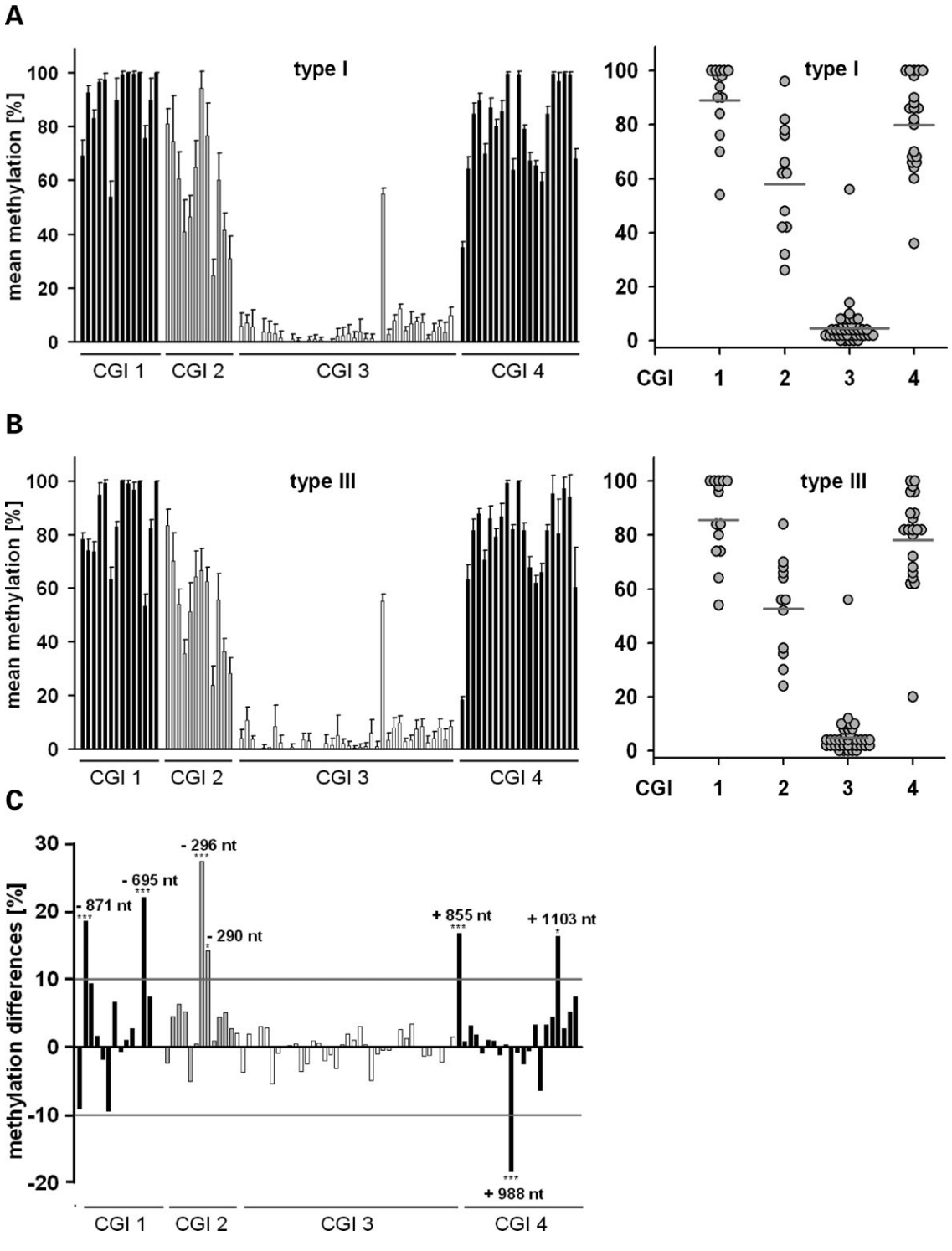


**Figure 3.** *Survival motor neuron gene 2* (*SMN2*) methylation patterns are highly conserved in blood samples derived from spinal muscular atrophy (SMA) patients. Bar charts show the mean methylation levels (±SEM) of each CpG dinucleotide within the respective $^{SMN2}$CGIs in DNA isolated from blood samples drawn from *SMN1*-deleted SMA patients carrying two *SMN2* copies (**A**, **B**). Type I ($n = 10$) and type III SMA patients ($n = 7$) show highly conserved *SMN2* methylation patterns as can be deduced from the comparatively low SEM for the methylation levels of each CpG dinucleotide. The mean methylation levels of each $^{SMN2}$CGI (see frequency plot) in both groups are as follows: type I SMA – $^{SMN2}$CGI 1: 89.1%, $^{SMN2}$CGI 2: 58.0%, $^{SMN2}$CGI 3: 4.6%, $^{SMN2}$CGI 4: 79.9%; type III SMA – $^{SMN2}$CGI 1: 85.5%, $^{SMN2}$CGI 2: 52.6%, $^{SMN2}$CGI 3: 4.8%, $^{SMN2}$CGI 4: 78.1%. *SMN2* methylation correlates with the disease severity. Bar chart shows differences in DNA methylation at each CpG dinucleotide in type I versus type III SMA patients (**C**). Seven CpG dinucleotides (nt −871, −695, −296, −290, +855, +988, +1103) were identified whose methylation frequencies differ by at least 10% in type I versus type III SMA patients. Correlations between CpG methylation frequencies and disease severity reached levels of significance in all seven cases. Three levels of statistical significance were discriminated: $^{*}P < 0.05$, $^{**}P < 0.01$, $^{***}P < 0.001$ (*t*-test).

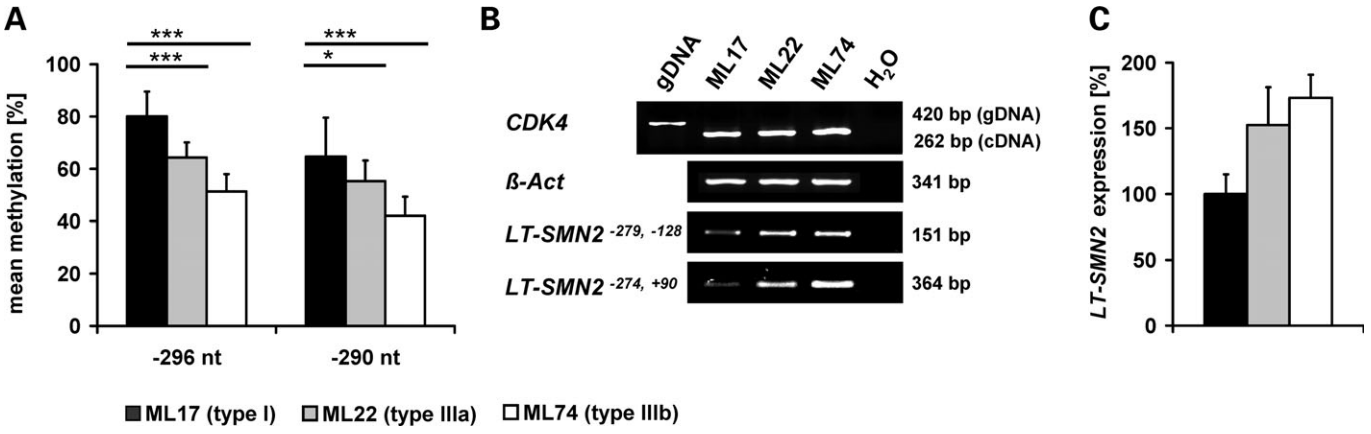


**Figure 4.** Low *survival motor neuron gene 2* (*SMN2*) methylation levels at the positions −296 and −290 are associated with mild spinal muscular atrophy (SMA) in SMA fibroblasts. (**A**) Bar chart showing the mean methylation levels (±SEM) at positions −296 and −290 in fibroblasts derived from *SMN1*-deleted SMA patients carrying two *SMN2* copies. At both sites, type I SMA fibroblasts (ML17) show significantly higher methylation levels than fibroblasts derived from type IIIa (ML22) and type IIIb (ML74) patients. Three levels of statistical significance were discriminated: $^{*}P < 0.05$, $^{**}P < 0.01$, $^{***}P < 0.001$ (*t*-test). Methylation levels at positions −296 and −290 correlate with the activity of the transcriptional start site (TSS) at position −296 in SMA fibroblasts. Relative to type I SMA fibroblasts (ML17), the low methylation levels at positions −296 and −290 observed in type IIIa and type IIIb SMA fibroblasts are associated with high *SMN2* transcripts levels originated from the TSS at position −296 (*LT-SMN2*) as shown by semi-quantitative RT–PCR analyses using two different primer combinations. (**B**) ß-Actin primers were used as internal control to verify equal loading of cDNA. *CDK4* primers were used to detect potential contaminations with genomic DNA (amplicon size cDNA: 262 bp, amplicon size gDNA: 420 bp). (**C**) Differences in *LT-SMN2* expression levels were confirmed by real-time PCR (normalized to ß-actin) using the $LT\text{-}SMN2^{-279,-128}$ primer pair. Data are given as mean percentage (±SEM) relative to *LT-SMN2* transcript levels in type I SMA fibroblasts (ML17) which were set to 100%.

### Reduced methylation at positions −296 and −290 of the *SMN2* gene is associated with mild SMA in SMA fibroblasts

To validate a correlation between *SMN2* gene methylation and the disease severity we analysed fibroblasts cell lines derived from independent *SMN1*-deleted SMA patients, also carrying two *SMN2* copies. Repeated quantification of CpG methylation levels at nt positions −296 and −290 (both $^{SMN2}$CGI 2) corroborated a significant correlation between CpG methylation and disease severity in type I (ML17), type IIIa (ML22) and type IIIb SMA fibroblasts (ML74) (Fig. 4A). No significant differences were observed at the remaining five positions (−871, −695, +855, +988, +1103, data not shown) demonstrated to be differentially methylated in DNA isolated from blood (Fig. 3C). Given the fact that the nearby CpG dinucleotides at nt positions −296 and −290 co-localize with the first TSS of *SMN2* located at nt position −296, it appears evident that methylation levels at these sites modulate the expression of *SMN2* transcripts derived from this TSS (subsequently designated as the *long transcript SMN2*, *LT-SMN2*). Using different primer combinations which specifically amplify *LT-SMN2*, an inverse correlation between −296 and −290 methylation levels and *LT-SMN2* transcript levels was observed in type I, type IIIa and type IIIb SMA fibroblast cell lines (Fig. 4B and C). However, no significant differences in total SMN2 protein levels were detected in ML17, ML22 and ML74 fibroblasts due to the finding that *LT-SMN2* transcripts account for <5% of total *SMN2* transcripts in these cells (data not shown).

### HDAC inhibitor treatment bypasses *LT-SMN2* gene silencing mediated by DNA methylation

Based on the observation that DNA methylation restricts *SMN2* gene activity (Fig. 1A and B), we hypothesized that the abolition of *SMN2* gene silencing conferred by DNA methylation might represent a promising strategy for pharmacologic SMA therapy. In 1998, Jones *et al*. (26) have shown that the experimental pan-HDAC inhibitor TSA is able to bypass gene silencing mediated by DNA methylation. To address this issue, type I SMA fibroblasts (ML17) showing high methylation levels at positions −296 and −290 associated with low *LT-SMN2* mRNA expression (Fig. 4) were treated with effective doses of highly potent HDAC inhibitors of different chemical classes. Specifically, cells were exposed to SAHA, M344, scriptaid, oxamflatin (hydroxamic acids), or romidepsin (FK-228, cyclic tetrapeptide) for 48 h. All five test compounds dramatically increased *LT-SMN2* transcript levels dose dependently, indicating that HDAC inhibitors are able to relieve *LT-SMN2* gene silencing mediated by DNA methylation (Fig. 5A and B). In all analyses, the dose-dependent inductions of *LT-SMN2* expression were associated with robustly increased total *SMN2* transcript levels. For example, treatment with 30 μM doses of SAHA results in a ∼25-fold induction of *LT-SMN2* and a 5-fold induction of total *SMN2* transcript levels (Fig. 5B). However, the hitherto analysed HDAC inhibitors possess negligible HDAC isoenzyme selectivities and concordantly we previously have shown that these compounds are able to fully antagonize HDAC activity *in vitro* (32). Thus, we next assessed whether isoenzyme selective HDAC inhibitors such as MS-275 as well as VPA and PB, which are both under clinical evaluation for SMA therapy, show similar effects. Interestingly, neither the benzamide MS-275 nor the fatty acids VPA and PB were able to substantially elevate *LT-SMN2* transcript levels even at excessive doses (Fig. 5B), indicating that MS-275, VPA and PB were not able to overcome *LT-SMN2* gene silencing conferred by DNA methylation in this experimental setting. To confirm these findings in a neuroectodermal tissue we subsequently employed human hippocampal brain

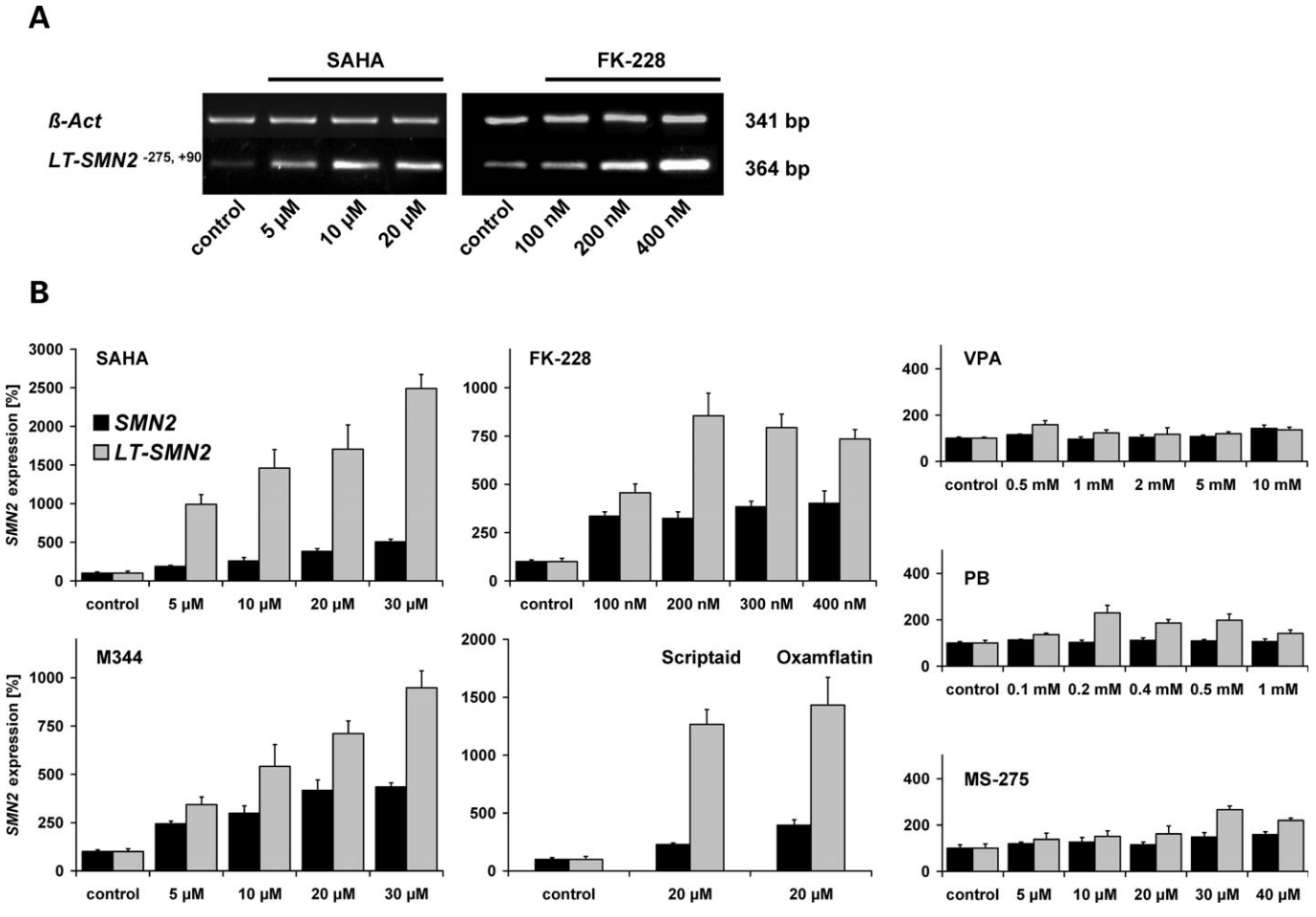


**Figure 5.** Histone deacetylase (HDAC) inhibitor treatment bypasses *LT-SMN2* gene silencing mediated by DNA methylation. Treatment of type I SMA (spinal muscular atrophy) fibroblasts (ML17) with increasing doses of SAHA (hydroxamic acid) or FK-228 (cyclic tetrapeptide) elevates *LT-SMN2* transcript levels in a dose-dependent manner as shown by semi-quantitative RT–PCR analyses. (**A**) ß-Actin primers were used as internal control to verify equal loading of cDNA. *LT-SMN2* and total *SMN2* transcript levels in type I SMA fibroblasts (ML17) following treatment with HDAC inhibitors for 48 h were further analysed by real-time PCR. (**B**) *LT-SMN2* and total *SMN2* transcript levels (both normalized to ß-actin) following HDAC inhibitor treatment are given as mean percentages (±SEM) relative to *LT-SMN2* and total *SMN2* transcript levels in solvent- and time-matched controls which were set to 100%.

slice cultures (OHSCs) derived from epilepsy surgery (four individuals, Fig. 6A–D). Even though *LT-SMN* transcripts derived from the *SMN1* or *SMN2* genes were not distinguishable in this experimental paradigm due to identical promoter sequences (33), a pronounced induction of *LT-SMN* transcription was observed following treatment with M344 (Fig. 6A) or SAHA (Fig. 6B and C), while VPA again had no or only moderate effects (Fig. 6B–D). A dose-dependent induction of SMN expression following treatment with M344 was confirmed on protein level (Fig. 6A).

### Transcriptional *LT-SMN2* induction by HDAC inhibitors is not mediated by DNA-demethylation of the *SMN2* gene

The mechanism by which pan-HDAC inhibitors such as SAHA and romidepsin (FK-228) bypass *LT-SMN2* silencing by DNA methylation remains elusive. In single cell cultures, TSA and VPA have shown to trigger DNA demethylation in a replication-independent manner (34–36) and gene-specific DNA demethylating activities of VPA, MS-275 and TSA have subsequently been confirmed *in vivo* (37,38). To assess whether HDAC inhibitors elevate *LT-SMN2* transcript levels due to their propensity to promote DNA demethylation, we next analysed the methylation levels of $^{SMN2}$CGI 2 in type I SMA fibroblasts (ML17) following HDAC inhibitor treatment for 48 h. Using 10 µM doses of SAHA, this experimental setting has shown to substantially elevate *LT-SMN2* and total *SMN2* transcript levels (Fig. 5A and B). However, SAHA did not promote $^{SMN2}$CGI 2 demethylation and neither did VPA or PB as shown by bisulphite genomic sequencing (Fig. 7A). In contrast, treatment of ML17 cells with zebularine, a DNA-demethylating drug structurally related to Aza, induced $^{SMN2}$CGI 2 demethylation (Fig. 7A and B), and consistent with previous findings, reduced $^{SMN2}$CGI 2 methylation levels including the nt positions −296 and −290 associated with significantly increased *LT-SMN2* transcript levels (Fig. 7B and C). These results suggest that transcriptional *LT-SMN2* induction by HDAC inhibitors is not mediated by DNA-demethylation of the *SMN2* gene promoter.

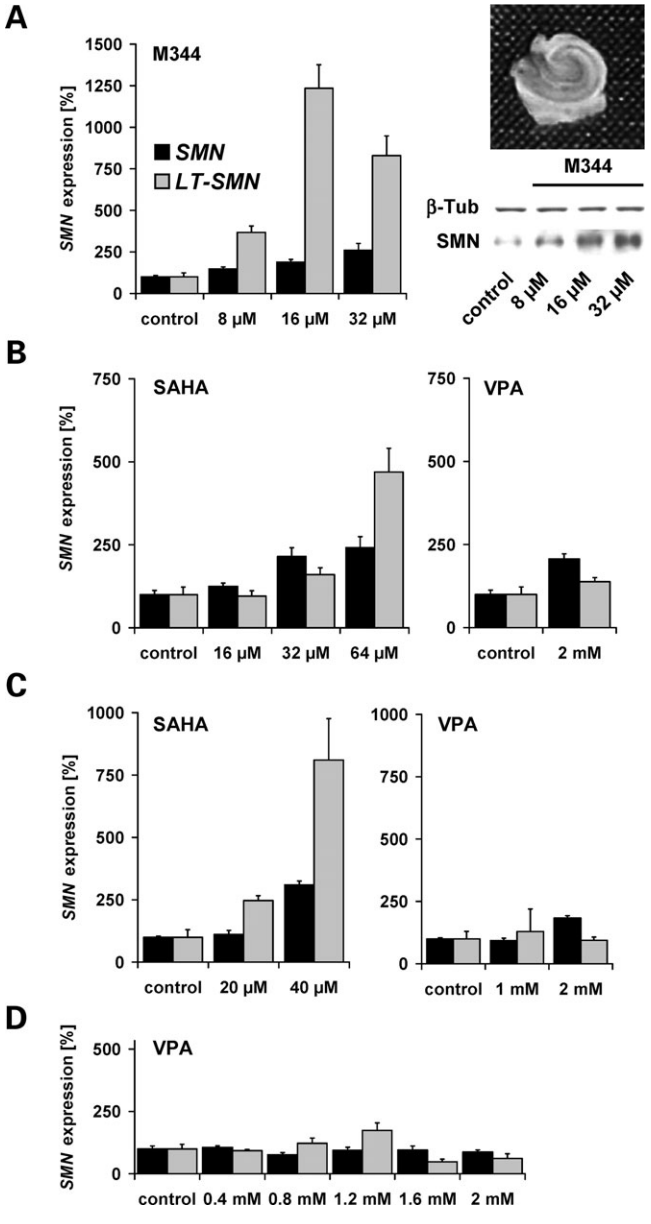


**Figure 6.** HDAC (histone deacetylase) inhibitor treatment elevates *LT-SMN* expression in human organotypic hippocampal brain slice cultures (OHSCs). (**A**–**D**) Bar charts showing *LT-SMN* and total survival motor neuron (*SMN*) transcript levels in human OHSCs derived from four different individuals. OHSCs were treated with the indicated doses of M344, SAHA or VPA (valproic acid) for 48 h. *LT-SMN* and total *SMN* transcript levels (both normalized to ß-actin) are given as mean percentages ($\pm$SEM) relative to *LT-SMN* and total *SMN* transcript levels in solvent- and time-matched controls which were set to 100%. Using OHSCs derived from the first patient (A), a dose-dependent *SMN* induction was confirmed on protein level (relative to ß-tubulin; 8 µM: 138 $\pm$ 2%; 16 µM: 188 $\pm$ 30%; 32 µM: 219 $\pm$ 41%). A representative human OHSC and a representative western blot analysis are shown. Induction of SMN protein expression by M344 reached levels of significance at all indicated doses ($P < 0.05$, *t*-test).

### Transcriptional repressor MeCP2 binds to the *SMN2* promoter and mediates transcriptional *LT-SMN2* silencing

Two basic models evolved regarding the mechanism by which DNA methylation affects transcription (39). DNA methylation can directly repress transcription by blocking transcriptional activators from binding to cognate DNA sequences, alternatively methyl-CpG DNA-binding proteins (MBPs) recognize methylated DNA and recruit co-repressors to silence gene expression directly. Since HDAC inhibitors do not promote *SMN2* gene demethylation in our experimental setting (Fig. 7A), and are able to bypass *LT-SMN2* gene silencing by DNA methylation (Figs 5 and 6), we hypothesized that DNA methylation at the *SMN2* promoter region is recognized by an MBP which recruits HDAC activity to mediate epigenetic gene silencing. Previous studies revealed that two global mechanisms of epigenetic gene regulation, DNA methylation and histone deacetylation, can be linked by the methyl-CpG-binding-protein 2 (MeCP2) (27). MeCP2 is an abundant chromosomal protein that specifically binds to methylated DNA and requires HDAC activity to repress transcription from methylated promoters (26,27). Thus, we hypothesized that the methylated *SMN2* promoter is recognized by MeCP2. In line with this hypothesis, siRNA-mediated knockdown of MeCP2 resulted in significantly increased *LT-SMN2* transcript levels in ML17 type I SMA fibroblast cells (Fig. 7D). To validate the role of MeCP2 in *LT-SMN2* expression, we next analysed the potential binding of MeCP2 to the *SMN2* promoter region by chromatin immunoprecipitation (ChIP). Initial analyses using $^{SMN2}$CGI 2-specific primers covering the genomic region from nt $-372$ to $-266$ revealed a clear association of MeCP2 with the *SMN2* promoter region in ML17 SMA fibroblasts (Fig. 7E). Elevated *LT-SMN2* transcript levels following treatment of ML17 fibroblasts with zebularine (Fig. 7C) are associated with a decrease in the MeCP2 binding to the *SMN2* promoter (Fig. 7F), indicating that MeCP2 recognizes the *SMN2* promoter in a methylation-dependent fashion. Moreover, increased *LT-SMN2* transcript levels following siRNA-mediated knockdown of MeCP2 (Fig. 7D) are associated with decreased MeCP2 binding to the *SMN2* promoter ($77.8 \pm 4.6\%$, $P < 0.05$, *t*-test). These data indicate a methylation-dependent binding of the transcriptional repressor MeCP2 to the *SMN2* promoter region resulting in *LT-SMN2* silencing. To determine the binding pattern of MeCP2 on the *SMN2* promoter we performed MeCP2 ChIP analyses using ML17 SMA fibroblasts and six different primer pairs covering the genomic *SMN2* promoter region from nt $-631$ to $+59$, which comprises $^{SMN2}$CGI 2 (nt $-469$ to $-247$) and adjacent sequences. Although MeCP2 binding was detectable in all cases (Fig. 7G), ChIP-PCR signal intensities were substantially higher at the genomic region from nt $-349$ and $-63$, suggesting enrichment at this site. This particular 286 bp region contains all three transcriptional *SMN2* start sites at positions $-296$, $-242$ and $-163$ and the differentially methylated CpG dinucleotides at positions $-296$ and $-290$, suggesting a probable role of MeCP2 in *SMN2* gene silencing.

## DISCUSSION

Here, we show for the first time that *SMN2*, the major disease modifier and target gene for pharmacological SMA treatment, is epigenetically regulated by DNA methylation given by the

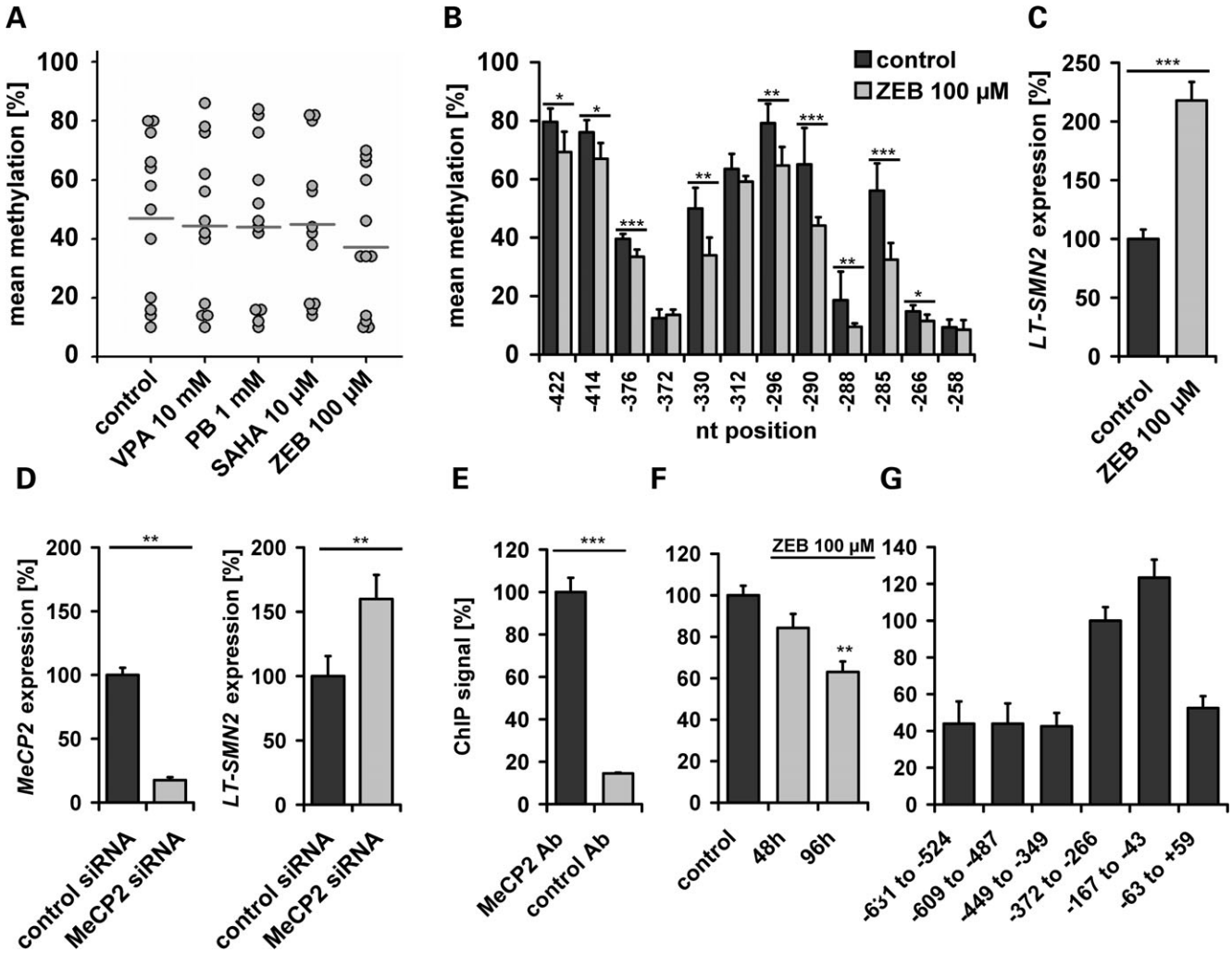


**Figure 7.** *LT-SMN2* induction by HDAC (histone deacetylase) inhibitors is not mediated by *survival motor neuron gene 2* (*SMN2*) promoter demethylation. (**A**) Treatment of type I spinal muscular atrophy (SMA) fibroblasts (ML17) with valproic acid (VPA) (10 mM), phenylbutyrate (PB) (1 mM) or SAHA (10 µM) for 48 h did not affect $^{SMN2}$CGI 2 methylation levels. Frequency plot illustrating methylation levels of each CpG dinucleotide within the $^{SMN2}$CGI 2 in treated ML17 cells compared with time- and solvent-matched ML17 control fibroblasts. The DNA-demethylating drug zebularine (ZEB, 100 µM) was used as positive control. The mean methylation levels of $^{SMN2}$CGI 2, indicated by horizontal lines, are as follows – control: 47.0%, VPA: 44.5%, PB 44.1%, SAHA: 45.0%, ZEB: 37.3%. Demethylation of CpG dinucleotides at positions −296 and −290 is associated with increased *LT-SMN2* expression. Treatment of type I SMA fibroblasts (ML17) with ZEB (100 µM, 48 h) results in a significant demethylation of nine out of 12 CpG dinucleotides located in $^{SMN2}$CGI 2, including the nt positions −296 and −290. (**B**) ZEB-induced $^{SMN2}$CGI 2 demethylation is associated with increased *LT-SMN2* levels as shown by quantitative real-time PCR. *LT-SMN2* transcript levels (normalized to ß-actin) are given as mean percentages (± SEM) relative to *LT-SMN2* expression levels in solvent- and time-matched controls set to 100%. (**C**) siRNA-mediated knockdown of *MeCP2* elevates *LT-SMN2* transcript levels in ML17 SMA fibroblasts. (**D**) *MeCP2* and *LT-SMN2* transcript levels (normalized to ß-actin) are given as mean percentages (± SEM) relative to *MeCP2* or *LT-SMN2* expression levels in time-matched controls transfected with AllStars negative control siRNA. The transcriptional co-repressor methyl-CpG-binding-protein 2 (MeCP2) is associated with the *SMN2* promoter region and binds in a methylation-dependent fashion. (**E**, **F**) Using *SMN1*-deleted SMA fibroblasts cells (ML17), a significant binding of MeCP2 to the *SMN2* promoter region was observed by chromatin immunoprecipitation (ChIP) analysis using an anti-MeCP2 antibody and primers amplifying the genomic *SMN2* promoter region from nt −372 to −266. An unrelated antibody (negative Ctrl IgG, rabbit, Diagenode) was used as negative control. Treatment of ML17 SMA fibroblast cells with 100 µM ZEB resulted in a significant reduction of MeCP2 binding to the *SMN2* promoter region. MeCP2 is enriched at a 286 bp *SMN2* promoter region. (**G**) ChIP analyses using ML17 fibroblasts and six different primer pairs covering the genomic *SMN2* promoter region from nt −631 to +59. Enrichment after MeCP2 ChIP was detectable for all primer pairs while two primer pairs showed considerably higher ChIP-PCR signal intensities. Three levels of statistical significance were discriminated: $^{*}P < 0.05$, $^{**}P < 0.01$, $^{***}P < 0.001$ (*t*-test).

fact that DNA-demethylating compounds increase *SMN2* gene activity (Figs 1A and B, and 7C). We demonstrate that *SMN2* contains four putative CGIs ($^{SMN2}$CGIs) located within the genomic region 896 nt upstream and 1146 nt downstream of its translational start site (Fig. 2A). Analysis of DNA isolated from fibroblast cell lines and blood samples derived from *SMN1*-deleted SMA patients identified $^{SMN2}$CGI 1 and $^{SMN2}$CGI 4 to be hypermethylated, $^{SMN2}$CGI 3 appeared to be almost methylation-free, while $^{SMN2}$CGI 2 showed intermediate methylation levels (Figs 2B and C, and 3A–C). Since CGIs are usually defined as short unmethylated DNA patches (29), solely $^{SMN2}$CGI 3 (446 bp, GC content 62.1%)

can be regarded as a 'classical' CGI. However, recent data categorize $^{SMN2}$CGI 1 (252 bp, GC content 54.8%), $^{SMN2}$CGI 2 (223 bp, GC content 58.3%) and $^{SMN2}$CGI 4 (303 bp, GC content 59.4%) as 'weak' CGIs due to their small size and comparatively low GC content (40). Differences between the 'classical' $^{SMN2}$CGI 3 and the 'weak' $^{SMN2}$CGIs 1, 2 and 4 become more apparent when calculating the CpG density, which is defined as the ratio between observed versus expected CpG dinucleotides (40). Although $^{SMN2}$CGI 3 possesses a high CpG density (0.94) usually found in unmethylated CGIs, the remaining $^{SMN2}$CGIs show intermediate CpG densities ($^{SMN2}$CGI 1: 0.74, $^{SMN2}$CGI 2: 0.79, $^{SMN2}$CGI 4: 0.79) characteristic for weak CGIs (29). In line with our data (Figs 2B and C, and 3A and B), weak CGIs usually show high frequencies of DNA methylation (40). Moreover, *SMN2* appears to be a typical gene regarding its CGI distribution. Approximately 70% of human genes are linked to promoter CGIs (41) and about half of all CGIs were found at the TSS of an annotated gene (such as $^{SMN2}$CGI 2) (29). Among the four $^{SMN2}$CGIs analysed, we provide first evidence that particularly the genomic region comprising the weak $^{SMN2}$CGI 2 is functionally important regarding SMA disease progression and pharmacological SMA therapy.

Even though *SMN2* has been identified as the major SMA disease modifier, differences in disease progression have frequently been observed in the presence of identical *SMN1* mutations and *SMN2* copy numbers (9,42). In the presence of two *SMN2* copies, homozygous absence of *SMN1* causes type I SMA in approximately two-thirds of all patients, while milder phenotypes are consequently also quite common (9,42). These findings led to the hypothesis that *SMN2* genes are not functionally equivalent. Using DNA derived from comparatively easily accessible sources such as blood and skin we identified significantly lower methylation levels at two adjacent CpG dinucleotides in type III SMA patients compared with patients suffering from severe type I SMA (nt positions −296 and −290, both $^{SMN2}$CGI 2, Figs 3C and 4A), suggesting that the capability of the *SMN2* gene copies to counteract SMA disease progression is modulated by DNA methylation. The functional relevance of DNA methylation at nt positions −296 and −290 is further highlighted by the finding that these CpG dinucleotides co-localize with the first TSS of *SMN2* at nt position −296 (Fig. 2A). We demonstrate that methylation levels at nt positions −296 and −290 inversely correlate with the activity of the first TSS of *SMN2* (Figs 4A–C, and 7B and C) indicating that DNA methylation at these nt positions is linked with transcriptional *LT-SMN2* silencing. In summary, our data provide first evidence that *SMN2* gene copies are not functionally equivalent due to differences in DNA methylation affecting *LT-SMN2* expression. However, *LT-SMN2* contributes only moderately to total *SMN2* transcript levels in SMA fibroblasts (described earlier). To address the question whether *LT-SMN2* expression is regulated in a tissue-dependent fashion, we subsequently quantified *LT-SMN2* and total *SMN2* transcript levels in various tissues derived from adult transgenic mice carrying the human *SMN2* gene ($Smn^{-/-}$ $SMN2^{+/+}$) (43). Consistent with previous findings, total *SMN2* transcript levels are higher in CNS tissues such as cerebrum and spinal cord compared with mesodermal and endodermal tissues such as skeletal muscle, heart and liver (19). Similarly, *LT-SMN2* transcripts display considerably higher expression levels in CNS tissues with a >3-fold higher expression in spinal cord compared with muscle, heart and liver, suggesting that the amounts of SMN protein derived from *LT-SMN2* are sufficient to modulate motor neuron degradation (Supplementary Material, Fig. S1). However, SMA disease severities appear to be modified by multiple mechanisms. In rare cases, haploidentical *SMN1*-deleted siblings show highly discordant SMA phenotypes ranging from affected to unaffected (44). In these families it has been shown that the SMA phenotype can be influenced by elevated expression of an independent modifying gene, *Plastin 3*, which protects against SMA in females (45). Exemplary analysis of nt positions −296 and −290 in two of these families (#34, #482) (44) revealed no differences in DNA methylation between haploidentical affected and unaffected individuals (data not shown).

Despite the apparent correlation between the CpG methylation levels at nt positions −296 and −290 and the disease severity, the finding that *LT-SMN2* expression is silenced by DNA methylation is especially important regarding pharmacological SMA therapy using HDAC inhibitors. The fundamental mechanisms of epigenetic gene regulation, DNA methylation and histone acetylation, have shown to be interlinked (26,27). Consistent with these findings we demonstrate that a panel of five pan-HDAC inhibitors including the hydoxamic acid vorinostat (SAHA) as well as the cyclic tetrapeptide romidepsin (FK-228) are able to bypass *LT-SMN2* gene silencing in SMA fibroblasts (Fig. 5) and human OHSCs (Fig. 6), resulting in up to 5-fold inductions of total *SMN2* transcript levels. In contrast, the HDAC isoenzyme selective inhibitors MS-275, VPA and PB display only moderate effects (Figs 5 and 6). These findings highlight functional differences between HDAC inhibitors regarding pharmacological SMA therapy and suggest that pan-HDAC inhibitors possess superior functional capacities to activate *SMN2*. Given the fact that the pan-HDAC inhibitors vorinostat (SAHA) and romidepsin (FK-228) are either FDA approved or under clinical phase II evaluation for cancer treatment, our data further highlight that these readily available compounds might be considered as candidate drugs for SMA therapy in case the ongoing clinical trials using VPA or PB do not show the desired efficacies. Especially vorinostat appears to be promising due to the fact that this molecule has shown to cross the blood-brain barrier and ongoing clinical evaluation in cancer patients exemplifies a good oral bioavailability and biological activity (46).

Moreover, we provide evidence of how *LT-SMN2* gene silencing by DNA methylation is regulated. ChIP experiments using ML17 SMA fibroblasts revealed that the methyl-CpG-binding protein 2 (MeCP2) is localized at a 286 bp *SMN2* promoter region (nt −349 to −63) containing all the three transcriptional *SMN2* start sites at nt positions −296, −242 and −163 as well as the differentially methylated CpG dinucleotides at positions −296 and −290 (Fig. 7G). MeCP2 binds to the *SMN2* promoter region in a methylation-dependent fashion (Fig. 7F) and MeCP2 knockdown induced *LT-SMN2* mRNA expression (Fig. 7D).

Following binding to methylated DNA, MeCP2 is known to recruit HDACs to chromatin (26,47), suggesting that the regulatory component MeCP2 might be involved in mediating *SMN2* gene silencing by DNA methylation. Since the isoenzyme selective HDAC inhibitors MS-275 and VPA have shown to inhibit HDAC1, HDAC2, HDAC3 (both MS-275 and VPA) and HDAC9 (MS-275) at doses used in our study (32), the finding that these drugs do not counteract *LT-SMN2* silencing suggests that the *LT-SMN2* induction observed following pan-HDAC inhibitor treatment was due to inhibition of the remaining classical HDACs (HDACs 4–8, 10, 11). Thus, further analysis of the specific roles of MeCP2 and HDAC isoenzymes in *LT-SMN2* expression represent important steps to develop optimized HDAC inhibitors targeted to overcome *LT-SMN2* silencing.

Regarding the apparent correlation between $^{SMN2}$CGI 2 methylation levels and disease severity, continuative studies are mandatory to assess whether the accurate quantification of DNA methylation levels at nt positions −296 and −290 represents a valuable tool to predict SMA disease progression in the presence of identical *SMN1* mutations and *SMN2* copy numbers. Furthermore, initial *SMN1* promoter methylation analyses of DNA samples derived from *SMN2*-deleted and unaffected individuals revealed that *SMN1* is subject to promoter methylation very similar to *SMN2* (Supplementary Material, Fig. S2). Based on these findings one might speculate whether aberrant *SMN1* promoter methylation may be causative for SMA in patients showing at least one non-mutated *SMN1* gene copy.

## MATERIALS AND METHODS

### Chemicals

The following chromatin-remodelling compounds have been used: M344 (382149, Calbiochem, San Diego, CA, USA), MS-275 (382147, Calbiochem), PB (567616, Calbiochem), zebularine (691400, Calbiochem), SAHA (270–288, Axxora, Lörrach, Germany), VPA (P-4543, Sigma-Aldrich, St Louis, MO, USA), scriptaid (S7817, Sigma-Aldrich), oxamflatin (O3139, Sigma-Aldrich) and Aza (A-3656, Sigma-Aldrich). Romidepsin (FK-228) was kindly provided by Gloucester Pharmaceuticals (Cambridge, MA, USA). All test compounds were dissolved in 100% DMSO or $H_2O$ (VPA).

### SMA patient samples and DNA isolation

Informed consent was obtained from all SMA patients or their parents. All patients fulfilled the diagnostic criteria for SMA (48); SMA disease severities (type I SMA, MIM #253300; type II SMA, MIM #253550; type IIIa/IIIb, MIM #253400) were classified as described (49). Genomic DNA was isolated from venous blood samples drawn for diagnostic purposes using the salting-out method (50) and *SMN1*/*SMN2* gene copy numbers were determined as described previously (9). The fibroblast cell lines used in this study have been established from skin biopsies and were cultured as described (14). Fibroblasts were cultured for the indicated time spans and harvested by trypsinization. DNA was isolated from fibroblast cell cultures using the QIAamp DNA Mini Kit (Qiagen, Hilden, Germany) according to the manufacturer's protocol.

### Human OHSCs

Human hippocampi were obtained from patients with chronic intractable temporal lobe epilepsy who underwent surgical treatment in the Epilepsy Surgery Program at the Department of Neurosurgery (University of Erlangen). For scientific use of tissue specimens, informed and written consent was obtained from all patients and studies were approved by the local Ethics Committee of the University of Erlangen. Surgical specimens were prepared and processed according to the interface technique (51). In brief, hippocampal brain samples were cut into 350 μm thick horizontal slices on a vibratome (Leica Microsystems, Wetzlar, Germany). Each brain slice was transferred into culture plate insert membranes (BD Biosciences, San Jose, CA, USA) and thereafter into 6-well culture dishes (BD Biosciences) containing 1.2 ml culture medium as described in detail (52). A day after preparation, culture medium was changed, human OHSCs were exposed to the test compounds or solvent only for 48 h and snap-frozen in liquid nitrogen.

### Protein sample preparation and western blot analysis

Human OHSCs and fibroblast cell culture cell pellets were resuspended in RIPA buffer (150 mM NaCl, 1% NP40, 0.5% DOC, 0.1% SDS, 50 mM Tris, pH 8.0) to obtain whole cell protein extracts. Denatured protein (7.5 μg) of each sample were resolved by SDS–PAGE on 4–12% Bis–Tris Gels (Invitrogen, Carlsbad, CA, USA) and transferred to nitrocellulose membrane by overnight wet blotting. Immunostaining of the membrane was performed according to standard protocols using the following antibodies: mouse monoclonal anti-ß-tubulin (T 4026, Sigma-Aldrich, dilution 1:20 000), mouse monoclonal anti-SMN (610647, BD Biosciences, dilution 1:1,000) and horseradish peroxidase conjugated goat anti-mouse IgG (115-035-003, Dianova, dilution 1:10 000) as secondary antibody. Detection of signals was carried out using the Super Signal West Pico chemiluminescence reagent (Pierce, Rockford, IL, USA). Densitometric analyses were performed using the Quantity One 1-D Analysis Software (Bio-Rad, Hercules, CA, USA).

### RNA isolation and quantitative RT–PCR analysis

Isolation of total RNA was performed using the RNeasy Mini Kit and QIAshredder columns according to the manufacture's protocol (Qiagen). RNA concentrations were determined spectrophotometrically. For semiquantitative PCR analyses, reverse transcription (RT) was performed using oligo dT primers and 1 μg of total RNA by applying the SuperScript First-Strand Synthesis System (Invitrogen). Two microlitres of each RT reaction was used for each RT–PCR. cDNAs were amplified using primers of *ß-actin* (ß-actin-fwd: 5′-AAC GGC TCC GGC ATG TGC AA-3′, ß-actin-rev: 5′-CTC AAA CAT GAT CTG GGT CAT CTT-3′), *CDK-4* (CDK-4-fwd: 5′-CTA TGG GAC AGT GTA CAA GG-3′, CDK-4-rev: 5′-GAT ATG TCC TTA GGT CCT GG-3′),

*LT-SMN2* (LT-SMN2$^{-279}$-fwd: 5′-ACT CCA GCC TGA GCG ACA-3′, LT-SMN2$^{-274}$-fwd: 5′-AGC CTG AGC GAC AGG GCGA-3′, LT-SMN2$^{-128}$-rev: 5′-TCT ACG AGT GGT TAT CGC-3′, LT-SMN2$^{+90}$-rev: 5′-ATC ATC GCT CTG GCC TGT GCC-3′). The following PCR conditions were used: 5 min initial denaturation (95°C), followed by 25–37 cycles (95°C for 15 s, 68°C for 30 s and 72°C for 35 s and final extension step (72°C for 5 min). PCR products were separated on 2% agarose gels and visualized by ethidium bromide staining. For real-time quantification of target gene expression, one step RT–PCR was preformed using the QuantiTect SYBR Green RT–PCR Kit (Qiagen) on an Applied Biosystems 7500 Real-Time PCR System (Applied Biosystems, Darmstadt, Germany). Each 20 μl RT–PCR mix contained 10 ng total RNA (4 ng/μl), 2 μl of the primer dilution, 10 μl ×2 QuantiTect SYBR Green RT-Master Mix and 0.2 μl QuantiTect RT Mix. One-step RT–PCR reactions were carried out in 96-well optical reaction plates, covered with Optical Adhensive Covers (Applied Biosystems). Cycling conditions were as follows: 50°C for 30 min (RT step), 95°C for 15 min and 40 cycles of 94°C for 15 s, 55°C for 30 s and 72°C for 35 s. Real-time RT–PCR was conducted four times for each gene and each RNA sample and results is given as mean ± SEM. The comparative method of relative quantification ($2^{-\Delta\Delta Ct}$) was used to calculate the relative expression levels of each target gene (normalized to ß-actin) compared with the non-treated control samples. RT–PCR specificity of each reaction was verified by melting curve analysis and confirmed by 2% agarose gel electrophoresis. Whenever possible, amplicons have been designed to span exon borders to exclude false positive detection of genomic contaminations. The following primers have been used for quantitative real-time RT–PCR: LT-SMN2-fwd 5′-ACT CCA GCC TGA GCG ACA-3′, LT-SMN2-rev 5′-TCT ACG AGT GGT TAT CGC-3′. *SMN2*: Quantitect primer assay QT01673679 (Qiagen), ß-actin: Quantitect primer assay QT00095431 (Qiagen), *MeCP2*: Quantitect primer assay QT00039361 (Qiagen). On cDNA level, full-length *SMN* transcripts derived from *SMN1* and *SMN2* are identical except for two silent nt differences in exons 7 and 8. *SMN2* Quantitect primer assay QT01673679 amplifies exons 5 and 6. Please note that the *SMN2* primers used also detect *SMN1* when present.

### Bisulphite genomic sequencing

DNA methylation analysis was carried out by bisulphite genomic sequencing using the pyrosequencing technology as described in detail (53). Bisulphite conversion of DNA (1 μg per sample) was performed using the EpiTect Bisulfite Kit (Qiagen) according to the manufacturer's protocol. Regions of interest were amplified by nested PCR using AmpliTaq Gold (Applied Biosystems) and biotinylated fwd/rev primer for the inner PCRs. The PCR conditions were as follows: 95°C for 5 min, followed by 40–50 cycles (95°C for 15 s, 52–55°C for 45 s, 72°C for 1 min) and a final extension step of 5 min at 72°C. The biotinylated PCR products (25 μl) were cleaned up using Streptavidin Sepharose™ High Performance (GE Healthcare, Uppsala, Sweden) and a PyroMark Vacuum Prep Workstation (Biotage, Uppsala, Sweden). The purified PCR products were used for the pyrosequencing reaction according to the manufacturer's protocol using Pyro Gold Reagents and the PSQ96 MA System (Biotage). Sequence analysis and quantification of CpG-dinucleotide methylation was performed using Pyro Q-CpG software (Biotage). Cloning of PCR products was performed using the TOPO TA Cloning Kit with One Shot TOP10 chemically competent *Escherichia coli* and the pcDNA3.1/V5-His Vector (Invitrogen). Plasmids of at least nine positive clones were isolated using the QIAprep Spin Miniprep Kit (Qiagen) according to the manufacturer's protocol. Inserts were sequenced using the BigDye Terminator Cycle Sequencing Kit V1.1 (Applied Biosystems) and the T7 forward primer. The primers used for bisulphite genomic sequencing (amplification, cloning, sequencing) are given in the Supplementary Material, Table S1. Please note that all primers given in the Supplementary Material, Table S1 detect *SMN1* and *SMN2* due to identical promoter sequences.

### siRNA-mediated knockdown of MeCP2

siRNA-mediated knockdown was performed as described previously (54). Briefly, 1 day before transfection $1 \times 10^5$ SMA fibroblast cells were plated out in each well of a 6-well culture dish. Cells were transfected with *MeCP2* siRNA (Qiagen, Hs_MeCP2_7, SI02664893, target sequence: ACG GAG CGG ATT GCA AAG CAA) or AllStars negative Control siRNA (Qiagen, 1027281) at a final concentration of 50 nM using DharmaFECT 1 siRNA Transfection Reagent (Dharmacon, Bonn, Germany). Transfection efficacy was controlled by transfection with siControl TOX transfection control (Dharmacon, D-001500-01-20). Cells were harvested after 48 h. RNA isolation and real-time PCR analyses were performed as described earlier.

### Chromatin immunoprecipitation

ChIP experiments were carried out using the LowCell# ChIP Kit (Diagenode, Liège, Belgium) according to the manufacturer's instructions. Briefly, $3 \times 10^5$ fibroblast cells were used for each analysis. Cells were harvested by trypsinization. Proteins were cross-linked to DNA by adding formaldehyde to a final concentration of 1% for 8 min at room temperature to the trypsinized cells. The fixation reaction was stopped by adding glycine to a final concentration of 0.125 M and subsequent incubation for 10 min at room temperature. Chromatin was sheared using a Bioruptor (Diagenode), utilizing maximum power for 15 min with 30 s on/off cycles at 4°C. Five microgram of the MeCP2 antibody (Diagenode) per reaction was bound to the Protein A-coated paramagnetic beads which were included in the Kit. One hundered microlitre of sheared chromatin were added to the antibody-coated paramagnetic beads and incubated overnight at 4°C with rotation. Chromatin was immunoprecipitated and washed by using a Magnetic Rack (Diagenode). Thereafter DNA was purified from the antibody coated beads by using DNA purifying slurry and incubation of the samples in boiling water for 10 min. This step was followed by addition of proteinase K (Diagenode) and incubation at 55°C for 30 min in a thermomixer (1000 rpm). Subsequently the samples were incubated again in boiling water for 10 min to elute the DNA. DNA

was analysed by real-time PCR on a 7500 Real-Time PCR System (Applied Biosystems), using Power SYBR Green PCR Master Mix (Applied Biosystems) and the primers listed in the Supplementary Material, Table S1. All PCRs were performed at least in triplicates.

## SUPPLEMENTARY MATERIAL

Supplementary Material is available at *HMG* Online.

*Conflict of Interest statement*. None declared.

## FUNDING

This work was kindly supported by the 'Initiative Forschung und Therapie für SMA' (to E.H. and to B.W.), the 'Köln Fortune Program/Faculty of Medicine, University of Cologne' (to E.H.), the 'Deutsche Forschungsgemeinschaft (DFG)' (to E.H., to I.B. and to B.W.), the 'Wilhelm Sander Foundation' (to E.H., I.Y.E. and I.B.), the 'Families of Spinal Muscular Atrophy' (to B.W. and E.H.) and the 'Center for Molecular Medicine Cologne' (to B.W. and E.H.). The 'Monash International Post graduate Research Scholarship (MIPRS)' and the 'Monash Graduate Scholarship (MGS)' (to S.L.). Funding to pay the Open Access charge was provided by the 'Initiative Forschung und Therapie für SMA'.

## REFERENCES

1. Wirth, B., Brichta, L. and Hahnen, E. (2006) Spinal muscular atrophy: from gene to therapy. *Semin. Pediatr. Neurol.*, **13**, 121–131.
2. Wirth, B. (2000) An update of the mutation spectrum of the survival motor neuron gene (SMN1) in autosomal recessive spinal muscular atrophy (SMA). *Hum. Mutat.*, **15**, 228–237.
3. Lefebvre, S., Burglen, L., Reboullet, S., Clermont, O., Burlet, P., Viollet, L., Benichou, B., Cruaud, C., Millasseau, P., Zeviani, M. *et al.* (1995) Identification and characterization of a spinal muscular atrophy-determining gene. *Cell*, **80**, 155–165.
4. Lorson, C.L., Hahnen, E., Androphy, E.J. and Wirth, B. (1999) A single nucleotide in the SMN gene regulates splicing and is responsible for spinal muscular atrophy. *Proc. Natl Acad. Sci. USA*, **96**, 6307–6311.
5. Lorson, C.L., Strasswimmer, J., Yao, J.M., Baleja, J.D., Hahnen, E., Wirth, B., Le, T., Burghes, A.H. and Androphy, E.J. (1998) SMN oligomerization defect correlates with spinal muscular atrophy severity. *Nat. Genet.*, **19**, 63–66.
6. Wolstencroft, E.C., Mattis, V., Bajer, A.A., Young, P.J. and Lorson, C.L. (2005) A non-sequence-specific requirement for SMN protein activity: the role of aminoglycosides in inducing elevated SMN protein levels. *Hum. Mol. Genet.*, **14**, 1199–1210.
7. Le, T.T., Pham, L.T., Butchbach, M.E., Zhang, H.L., Monani, U.R., Coovert, D.D., Gavrilina, T.O., Xing, L., Bassell, G.J. and Burghes, A.H. (2005) SMNDelta7, the major product of the centromeric survival motor neuron (SMN2) gene, extends survival in mice with spinal muscular atrophy and associates with full-length SMN. *Hum. Mol. Genet.*, **14**, 845–857.
8. McAndrew, P.E., Parsons, D.W., Simard, L.R., Rochette, C., Ray, P.N., Mendell, J.R., Prior, T.W. and Burghes, A.H. (1997) Identification of proximal spinal muscular atrophy carriers and patients by analysis of SMNT and SMNC gene copy number. *Am. J. Hum. Genet.*, **60**, 1411–1422.
9. Feldkotter, M., Schwarzer, V., Wirth, R., Wienker, T.F. and Wirth, B. (2002) Quantitative analyses of SMN1 and SMN2 based on real-time lightCycler PCR: fast and highly reliable carrier testing and prediction of severity of spinal muscular atrophy. *Am. J. Hum. Genet.*, **70**, 358–368.
10. Wirth, B., Brichta, L., Schrank, B., Lochmuller, H., Blick, S., Baasner, A. and Heller, R. (2006) Mildly affected patients with spinal muscular atrophy are partially protected by an increased SMN2 copy number. *Hum. Genet.*, **119**, 422–428.
11. Brahe, C. (2000) Copies of the survival motor neuron gene in spinal muscular atrophy: the more, the better. *Neuromuscul. Disord.*, **10**, 274–275.
12. Monani, U.R., Coovert, D.D. and Burghes, A.H. (2000) Animal models of spinal muscular atrophy. *Hum. Mol. Genet.*, **9**, 2451–2457.
13. Sumner, C.J., Huynh, T.N., Markowitz, J.A., Perhac, J.S., Hill, B., Coovert, D.D., Schussler, K., Chen, X., Jarecki, J., Burghes, A.H. *et al.* (2003) Valproic acid increases SMN levels in spinal muscular atrophy patient cells. *Ann. Neurol.*, **54**, 647–654.
14. Brichta, L., Hofmann, Y., Hahnen, E., Siebzehnrubl, F.A., Raschke, H., Blumcke, I., Eyupoglu, I.Y. and Wirth, B. (2003) Valproic acid increases the SMN2 protein level: a well-known drug as a potential therapy for spinal muscular atrophy. *Hum. Mol. Genet.*, **12**, 2481–2489.
15. Hahnen, E., Eyupoglu, I.Y., Brichta, L., Haastert, K., Trankle, C., Siebzehnrubl, F.A., Riessland, M., Holker, I., Claus, P., Romstock, J. *et al.* (2006) *In vitro* and *ex vivo* evaluation of second-generation histone deacetylase inhibitors for the treatment of spinal muscular atrophy. *J. Neurochem.*, **98**, 193–202.
16. Andreassi, C., Angelozzi, C., Tiziano, F.D., Vitali, T., De Vincenzi, E., Boninsegna, A., Villanova, M., Bertini, E., Pini, A., Neri, G. *et al.* (2004) Phenylbutyrate increases SMN expression in vitro: relevance for treatment of spinal muscular atrophy. *Eur. J. Hum. Genet.*, **12**, 59–65.
17. Chang, J.G., Hsieh-Li, H.M., Jong, Y.J., Wang, N.M., Tsai, C.H. and Li, H. (2001) Treatment of spinal muscular atrophy by sodium butyrate. *Proc. Natl Acad. Sci. USA*, **98**, 9808–9813.
18. Riessland, M., Brichta, L., Hahnen, E. and Wirth, B. (2006) The benzamide M344, a novel histone deacetylase inhibitor, significantly increases SMN2 RNA/protein levels in spinal muscular atrophy cells. *Hum. Genet.*, **120**, 101–110.
19. Kernochan, L.E., Russo, M.L., Woodling, N.S., Huynh, T.N., Avila, A.M., Fischbeck, K.H. and Sumner, C.J. (2005) The role of histone acetylation in SMN gene expression. *Hum. Mol. Genet.*, **14**, 1171–1182.
20. Avila, A.M., Burnett, B.G., Taye, A.A., Gabanella, F., Knight, M.A., Hartenstein, P., Cizman, Z., Di Prospero, N.A., Pellizzoni, L., Fischbeck, K.H. *et al.* (2007) Trichostatin A increases SMN expression and survival in a mouse model of spinal muscular atrophy. *J. Clin. Invest.*, **117**, 659–671.
21. Tsai, L.K., Tsai, M.S., Lin, T.B., Hwu, W.L. and Li, H. (2006) Establishing a standardized therapeutic testing protocol for spinal muscular atrophy. *Neurobiol. Dis.*, **24**, 286–295.
22. Mercuri, E., Bertini, E., Messina, S., Pelliccioni, M., D'Amico, A., Colitto, F., Mirabella, M., Tiziano, F.D., Vitali, T., Angelozzi, C. *et al.* (2004) Pilot trial of phenylbutyrate in spinal muscular atrophy. *Neuromuscul. Disord.*, **14**, 130–135.
23. Brahe, C., Vitali, T., Tiziano, F.D., Angelozzi, C., Pinto, A.M., Borgo, F., Moscato, U., Bertini, E., Mercuri, E. and Neri, G. (2005) Phenylbutyrate increases SMN gene expression in spinal muscular atrophy patients. *Eur. J. Hum. Genet.*, **13**, 256–259.
24. Weihl, C.C., Connolly, A.M. and Pestronk, A. (2006) Valproate may improve strength and function in patients with type III/IV spinal muscle atrophy. *Neurology*, **67**, 500–501.
25. Brichta, L., Holker, I., Haug, K., Klockgether, T. and Wirth, B. (2006) In vivo activation of SMN in spinal muscular atrophy carriers and patients treated with valproate. *Ann. Neurol.*, **59**, 970–975.
26. Jones, P.L., Veenstra, G.J., Wade, P.A., Vermaak, D., Kass, S.U., Landsberger, N., Strouboulis, J. and Wolffe, A.P. (1998) Methylated DNA and MeCP2 recruit histone deacetylase to repress transcription. *Nat. Genet.*, **19**, 187–191.
27. Nan, X., Ng, H.H., Johnson, C.A., Laherty, C.D., Turner, B.M., Eisenman, R.N. and Bird, A. (1998) Transcriptional repression by the methyl-CpG-binding protein MeCP2 involves a histone deacetylase complex. *Nature*, **393**, 386–389.
28. Eckhardt, F., Lewin, J., Cortese, R., Rakyan, V.K., Attwood, J., Burger, M., Burton, J., Cox, T.V., Davies, R., Down, T.A. *et al.* (2006) DNA methylation profiling of human chromosomes 6, 20 and 22. *Nat. Genet.*, **38**, 1378–1385.
29. Suzuki, M.M. and Bird, A. (2008) DNA methylation landscapes: provocative insights from epigenomics. *Nat. Rev. Genet.*, **9**, 465–476.

30. Monani, U.R., McPherson, J.D. and Burghes, A.H. (1999) Promoter analysis of the human centromeric and telomeric survival motor neuron genes (SMNC and SMNT). *Biochim. Biophys. Acta*, **1445**, 330–336.
31. Rouget, R., Vigneault, F., Codio, C., Rochette, C., Paradis, I., Drouin, R. and Simard, L.R. (2005) Characterization of the survival motor neuron (SMN) promoter provides evidence for complex combinatorial regulation in undifferentiated and differentiated P19 cells. *Biochem. J.*, **385**, 433–443.
32. Hahnen, E., Hauke, J., Trankle, C., Eyupoglu, I.Y., Wirth, B. and Blumcke, I. (2008) Histone deacetylase inhibitors: possible implications for neurodegenerative disorders. *Expert. Opin. Investig. Drugs*, **17**, 169–184.
33. Boda, B., Mas, C., Giudicelli, C., Nepote, V., Guimiot, F., Levacher, B., Zvara, A., Santha, M., LeGall, I. and Simonneau, M. (2004) Survival motor neuron SMN1 and SMN2 gene promoters: identical sequences and differential expression in neurons and non-neuronal cells. *Eur. J. Hum. Genet.*, **12**, 729–737.
34. Cervoni, N. and Szyf, M. (2001) Demethylase activity is directed by histone acetylation. *J. Biol. Chem.*, **276**, 40778–40787.
35. Detich, N., Bovenzi, V. and Szyf, M. (2003) Valproate induces replication-independent active DNA demethylation. *J. Biol. Chem.*, **278**, 27586–27592.
36. Milutinovic, S., D'Alessio, A.C., Detich, N. and Szyf, M. (2007) Valproate induces widespread epigenetic reprogramming which involves demethylation of specific genes. *Carcinogenesis*, **28**, 560–571.
37. Dong, E., Guidotti, A., Grayson, D.R. and Costa, E. (2007) Histone hyperacetylation induces demethylation of reelin and 67-kDa glutamic acid decarboxylase promoters. *Proc. Natl Acad. Sci. USA*, **104**, 4676–4681.
38. Weaver, I.C., Cervoni, N., Champagne, F.A., D'Alessio, A.C., Sharma, S., Seckl, J.R., Dymov, S., Szyf, M. and Meaney, M.J. (2004) Epigenetic programming by maternal behavior. *Nat. Neurosci.*, **7**, 847–854.
39. Klose, R.J. and Bird, A.P. (2006) Genomic DNA methylation: the mark and its mediators. *Trends Biochem. Sci.*, **31**, 89–97.
40. Weber, M., Hellmann, I., Stadler, M.B., Ramos, L., Paabo, S., Rebhan, M. and Schubeler, D. (2007) Distribution, silencing potential and evolutionary impact of promoter DNA methylation in the human genome. *Nat. Genet.*, **39**, 457–466.
41. Saxonov, S., Berg, P. and Brutlag, D.L. (2006) A genome-wide analysis of CpG dinucleotides in the human genome distinguishes two distinct classes of promoters. *Proc. Natl Acad. Sci. USA*, **103**, 1412–1417.
42. Cusco, I., Barcelo, M.J., Rojas-Garcia, R., Illa, I., Gamez, J., Cervera, C., Pou, A., Izquierdo, G., Baiget, M. and Tizzano, E.F. (2006) SMN2 copy number predicts acute or chronic spinal muscular atrophy but does not account for intrafamilial variability in siblings. *J. Neurol.*, **253**, 21–25.
43. Hsieh-Li, H.M., Chang, J.G., Jong, Y.J., Wu, M.H., Wang, N.M., Tsai, C.H. and Li, H. (2000) A mouse model for spinal muscular atrophy. *Nat. Genet.*, **24**, 66–70.
44. Hahnen, E., Forkert, R., Marke, C., Rudnik-Schoneborn, S., Schonling, J., Zerres, K. and Wirth, B. (1995) Molecular analysis of candidate genes on chromosome 5q13 in autosomal recessive spinal muscular atrophy: evidence of homozygous deletions of the SMN gene in unaffected individuals. *Hum. Mol. Genet.*, **4**, 1927–1933.
45. Oprea, G.E., Krober, S., McWhorter, M.L., Rossoll, W., Muller, S., Krawczak, M., Bassell, G.J., Beattie, C.E. and Wirth, B. (2008) Plastin 3 is a protective modifier of autosomal recessive spinal muscular atrophy. *Science*, **320**, 524–527.
46. Marks, P.A., Richon, V.M., Miller, T. and Kelly, W.K. (2004) Histone deacetylase inhibitors. *Adv. Cancer. Res.*, **91**, 137–168.
47. Harikrishnan, K.N., Chow, M.Z., Baker, E.K., Pal, S., Bassal, S., Brasacchio, D., Wang, L., Craig, J.M., Jones, P.L., Sif, S. *et al.* (2005) Brahma links the SWI/SNF chromatin-remodeling complex with MeCP2-dependent transcriptional silencing. *Nat. Genet.*, **37**, 254–264.
48. Munsat, T.L. and Davies, K.E. (1992) International SMA consortium meeting. (26–28 June 1992, Bonn, Germany). *Neuromuscul. Disord.*, **2**, 423–428.
49. Zerres, K. and Rudnik-Schoneborn, S. (1995) Natural history in proximal spinal muscular atrophy. Clinical analysis of 445 patients and suggestions for a modification of existing classifications. *Arch. Neurol.*, **52**, 518–523.
50. Miller, S.A., Dykes, D.D. and Polesky, H.F. (1988) A simple salting out procedure for extracting DNA from human nucleated cells. *Nucleic Acids Res.*, **16**, 1215.
51. Stoppini, L., Buchs, P.A. and Muller, D. (1991) A simple method for organotypic cultures of nervous tissue. *J. Neurosci. Methods*, **37**, 173–182.
52. Eyupoglu, I.Y., Hahnen, E., Buslei, R., Siebzehnrubl, F.A., Savaskan, N.E., Luders, M., Trankle, C., Wick, W., Weller, M., Fahlbusch, R. *et al.* (2005) Suberoylanilide hydroxamic acid (SAHA) has potent anti-glioma properties *in vitro*, *ex vivo* and *in vivo*. *J. Neurochem.*, **93**, 992–999.
53. Dupont, J.M., Tost, J., Jammes, H. and Gut, I.G. (2004) De novo quantitative bisulfite sequencing using the pyrosequencing technology. *Anal. Biochem.*, **333**, 119–127.
54. Brichta, L., Garbes, L., Jedrzejowska, M., Grellscheid, S.N., Holker, I., Zimmermann, K. and Wirth, B. (2008) Nonsense-mediated messenger RNA decay of survival motor neuron 1 causes spinal muscular atrophy. *Hum. Genet.*, **123**, 141–153.